POLYPROPYLENE CRYSTALLIZATION ON MALEATED POLYPROPYLENE-TREATED WOOD SURFACES: EFFECTS ON INTERFACIAL ADHESION IN WOOD POLYPROPYLENE COMPOSITES

Paul C. Kolosick*, George E. Myers** and James A. Koutsky*
* University of Wisconsin-Madison, Chemical Engineering Department, Madison, WI
** USDA Forest Products Laboratory, Madison, WI

ABSTRACT

Polypropylene (PP)-wood veneer laminates were used as a model system to investigate adhesion in wood-polypropylene composites. Wood veneers were treated with maleated polypropylene waxes (MA-PP). PP films were then compression molded to the wood surfaces and peel forces were measured.

Low MA-PP treatment levels increased the peel adhesion over that for untreated surfaces. High MA-PP treatment levels decreased the peel adhesion and intermediate MA-PP levels had no effect on the peel adhesion. Microscopy of the fracture surfaces indicated PP penetration into lumens in both treated and untreated wood veneer. Untreated surfaces also exhibited PP penetration into pits and intercellular spaces, while treated surfaces exhibited only hindered penetration on this scale. The penetrated PP formed tendrils during fracture. DSC of PP on wood and cellulose surfaces showed higher PP crystallization temperatures on untreated surfaces than on treated surfaces.

INTRODUCTION

Recent interest in lignocellulosic-polypropylene composites is well documented [1-3]. One area of special interest for these systems is the use of coupling agents. The nature of the two components, hydrophilic lignocellulosics and hydrophobic polypropylenes, suggests the need for coupling agents to improve interfacial adhesion and stress transfer between the two components. One type of coupling agent potentially useful for these systems is maleated-polypropylenes. In fact maleated-polypropylene waxes have been shown to improve the mechanical properties (tensile strength, bending strength, and impact strength) of extruded mixtures of wood-flour and polypropylene [4,5].

Our interest has been to develop a system which will allow for the characterization of the adhesion between lignocellulosics and polypropylene. An understanding of the adhesive mechanisms involved and how these mechanisms are affected by coupling agents will allow for the rational design of filler-coupling agent systems. Here we present a study of the effects of maleated-polypropylene on the adhesion between Birch and polypropylene using the model system we have developed.

EXPERIMENTAL

Two sets of experiments were done to evaluate the effects of a maleated-polypropylene wax on adhesion between birch and polypropylene. The first experiment (Experiment A) was a peel fracture test of PP-laminated Birch veneer. This test gave a direct measure of the overall adhesive force in the laminated system. In addition the fracture surfaces were investigated using Scanning Electron Microscopy (SEM). The second experiment (Experiment

 ©1992 Materials Research Society

B) used Differential Scanning Calorimetry (DSC) to investigate PP crystallization in the presence of Birch.

MATERIALS

The maleated-polypropylene (MA-PP) was emulsified Eastman E43, Eastman Chemical Co., with a number average molecular weight of 4500 and an acid number of 47 mg KOH/g polymer. The polypropylene (PP) was Soltex Fortilene 9101 homopolymer spheres with a density of 0.900 g/ml and a number average molecular weight of 76,000. The Birch was Yellow Birch (Betula alleghaniensis) knife-cut veneer.

EXPERIMENT A

Peel Tests

The veneer sheets (180 mm x 180 mm x 3 mm) were spray-coated with a water emulsion of the maleated-polypropylene wax (MA-PP) at four treatment levels (0.1, 0.4, 1.2 and 1.5 g/sheet). Control sheets were sprayed with distilled water. The treated sheets were then dried in a vacuum oven at 70°C for 2 hours. Extruded PP film (1.5 mm thick) was then laminated onto the veneer sheets in a Carver press. The press was operated at 175°C and 0.3 MPa with pressing times of 3 and 6 minutes. Each laminated sheet was then cut, parallel to the grain, into 6 strips (25 mm x 180 mm x 3 mm). The force required to peel the PP film off each strip was then measured using a 90° peel test. Reported peel forces for a given laminate are the average over the length of the 6 strips. The measuring procedure is described in detail elsewhere. [6]

Microscopy

The fracture surfaces resulting from the 90" peel tests were examined using Scanning Electron Microscopy (SEM). Representative micrographs of the surfaces were recorded. Qualitative values of the frequency of occurrence of various features were also noted.

EXPERIMENT B

Differential Scanning Calorimetry

PP crystallization in the presence of treated and untreated birch was examined using Differential Scanning Calorimetry (DSC). Birch powder (40-mesh) was prepared in a Wiley mill. The powder was prepared from the same veneer panels that were used for the peel samples. One half of the powder was treated with the emulsified MA-PP that was used in the peel tests. A mixture of the Birch powder and PP was melt-pressed into sheets using a Carver press at 0.3 MPa for 3 minutes. Samples (approximately 10 mg) were then cut from these sheets and analyzed. A typical DSC scan was run from 30°C to 200°C, held at 200°C for two minutes and then run from 200°C to 50°C. The heating and cooling steps were performed at 10°C/min.

RESULTS AND DISCUSSION

PEEL TEST RESULTS

The results of the 90° peel tests are shown in figure 1. The only improvement in peel force seen was for the lowest MA-PP level (0.1 g/sheet) and the highest press time (6 minutes). For this case the peel strength was 50% higher than for the untreated surface. In all the other cases there was no improvement over the untreated samples, and in the case of the highest MA-PP level (1.5 g/sheet) there was a significant decrease (55-70% decrease) in peel strength.

These results suggest the existence of an optimum MA-PP treatment level for this system. One interesting feature of this optimum is that it only occurs in the lowest treatment level at the highest press time. This suggest that the thickness of the MA-PP layer is important. The longer press time should allow for greater spreading of the MA-PP than the shorter press time. This would result in a thinner layer of MA-PP.

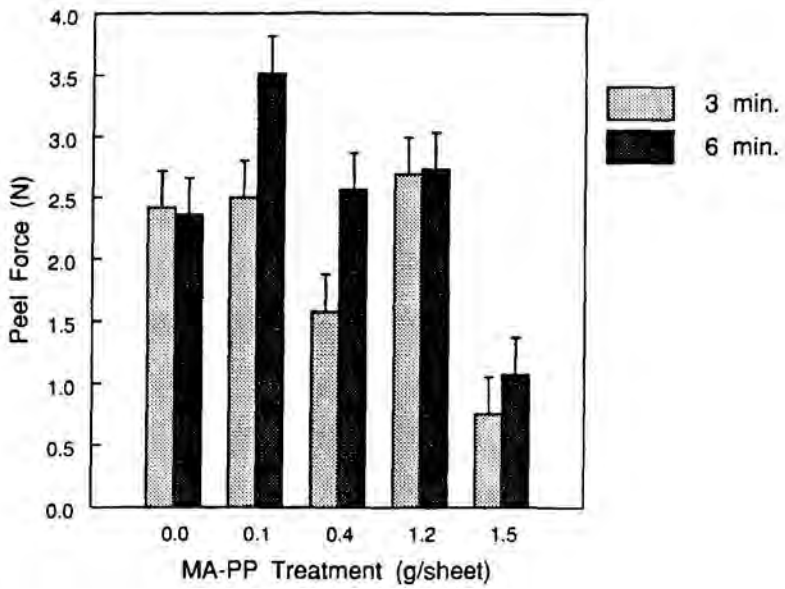

Figure 1 90° peel test results. MA-PP treated Birch veneer.

MICROSCOPY RESULTS

Scanning electron micrographs of the peel fracture surfaces are shown in figures 3 - 24. There are several important features to note:

(1) There are three effective "pore" sizes potentially available to the polypropylene. These are vessel lumens (30-60 microns), ray cells (~ 10 microns) and pits and intercellular spaces (~ 2 microns). Figure 2 shows the relative positions of these pores in the veneer.

(2) There is evidence of significant PP penetration into all three pore sizes in untreated veneer. See figures 4-6.

(3) Penetrated PP exhibits plastic deformation during the peel fracture. See figure 4-6.

(4) Pits and intercellular spaces are generally blocked to PP penetration in all the treated surfaces. They are almost totally blocked except in the 0.1 g/sheet - 6 minute case. See figures 11, 13, 17, 18, 23 and 24.

(5) Ray cells are partially blocked to PP penetration for the highest MA-PP treatment level (1.5 g/sheet). See figures 21 and 22.

(6) Some vessels are partially blocked to PP penetration in the 1.5 g/sheet cases. See figures 16 and 24.

(7) MA-PP generally exhibits brittle fracture. This is especially pronounced in relatively thick layers. See figure 20.

(8) There is evidence of chemical adhesion in the wood-MA-PP-polypropylene system for thin MA-PP layers, resulting in PP yielding at the MA-PP interface. See figures 10, 13 and 14.

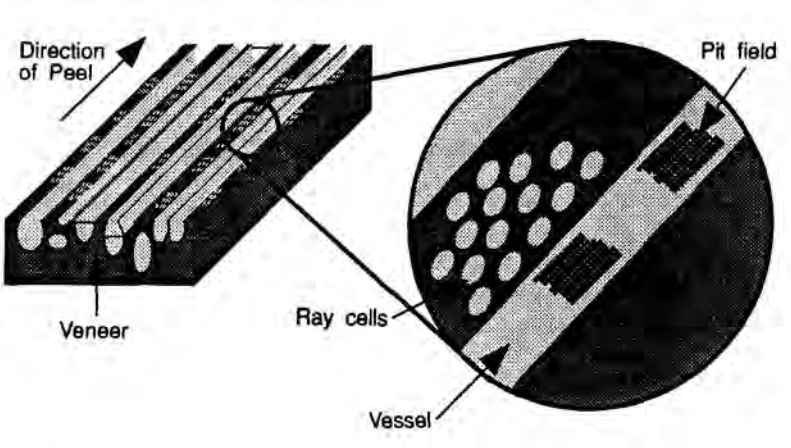

Figure 2: Veneer structure illustrating relative positions of vessels, ray cells and pit fields.

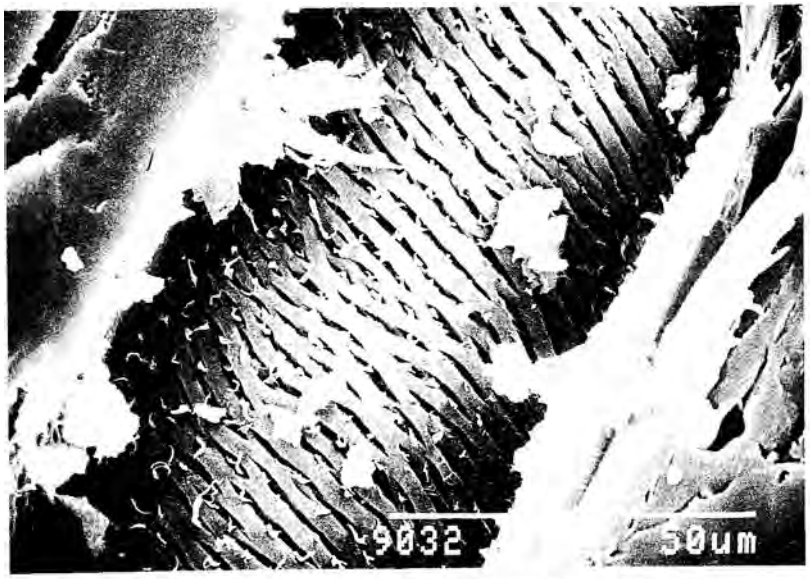

Figure 3: Untreated Birch ,0.3 MPa, 6 min., veneer side of failure.
Open vessel parallel to veneer surface. Note the pit field with PP tendrils extending through the pits.

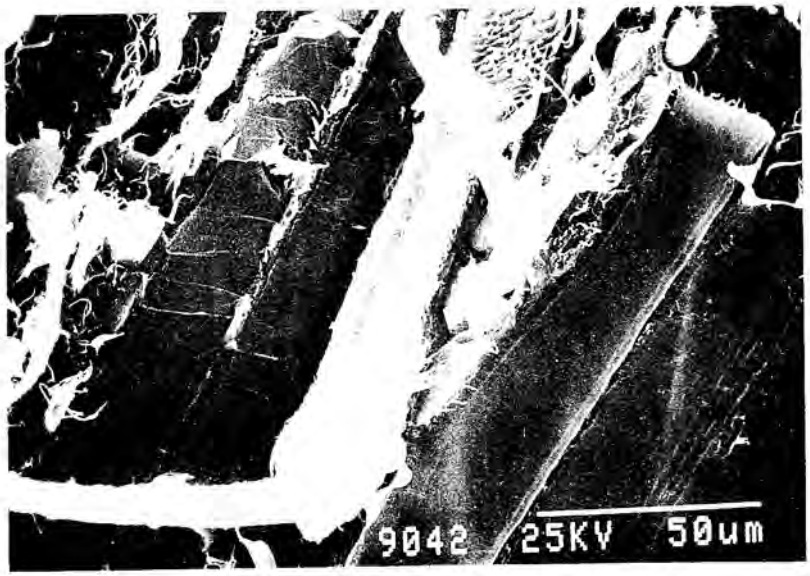

Figure 4: Untreated Birch, 0.3 MPa, 6 min., PP side of failure.
Vessel casting. Note PP tendrils extending from pit field on vessel casting. Also note necking of vessel casting.

Figure 5: Untreated Birch, 0.3 MPa, 6 min., PP side of failure.
PP tendrils pulled from ray cells. Note smaller tendrils resulting from PP penetration into intercellular spaces.

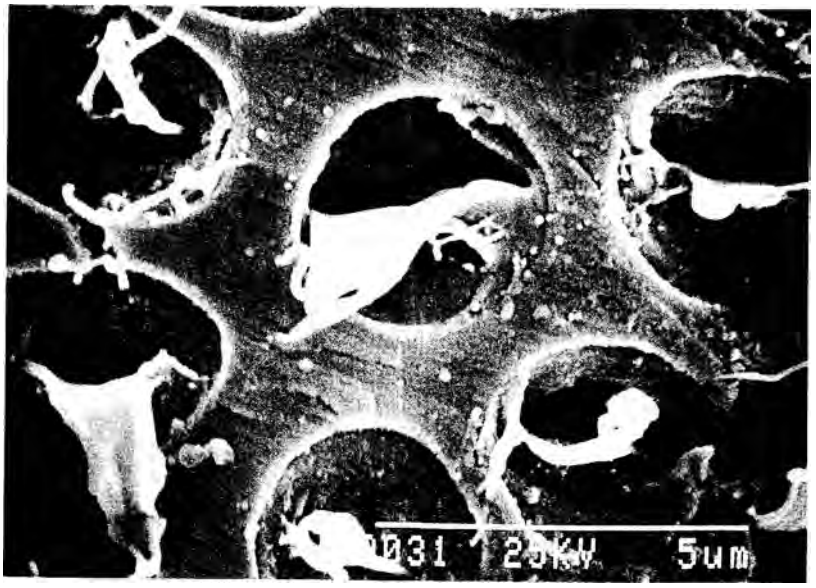

Figure 6: Untreated Birch, 0.3 MPa, 6 min., veneer side of failure.
Close-up of pit field (outside of vessel). Note PP tendrils pulled through pits.

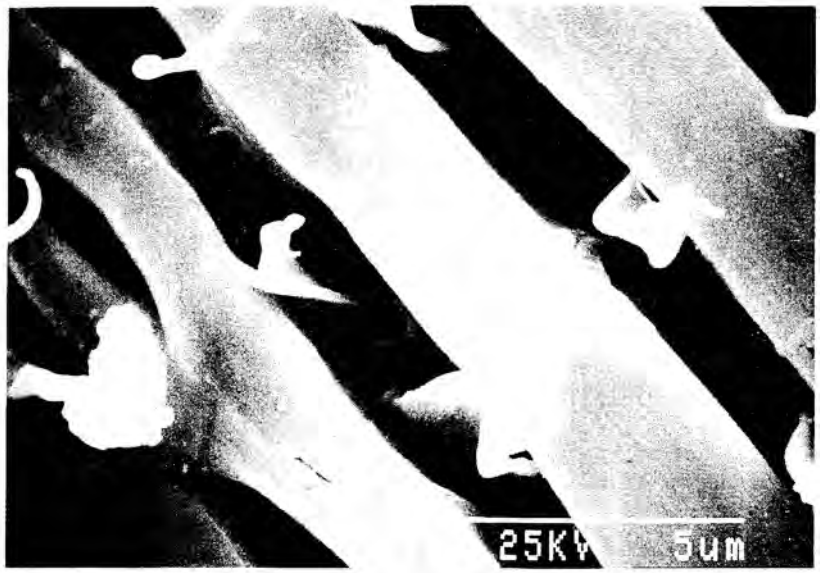

Figure 7: Untreated Birch, 0.3 MPa, 6 min., veneer side of failure. Close-up of pit field (inside of vessel). Note PP tendrils and clean lines of the pit field.

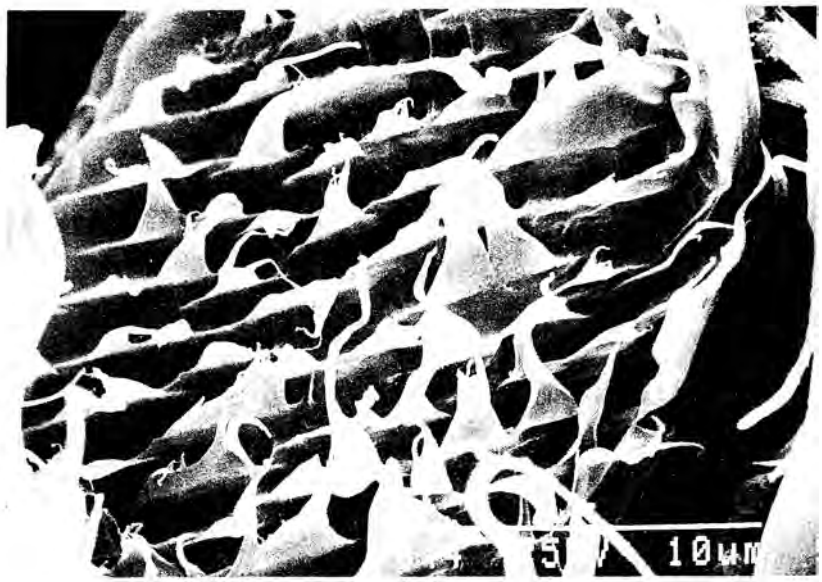

Figure 8: Untreated Birch, 0.3 MPa, 6 min., PP side of failure. Close-up of vessel casting. Note PP tendrils pulled from pits.

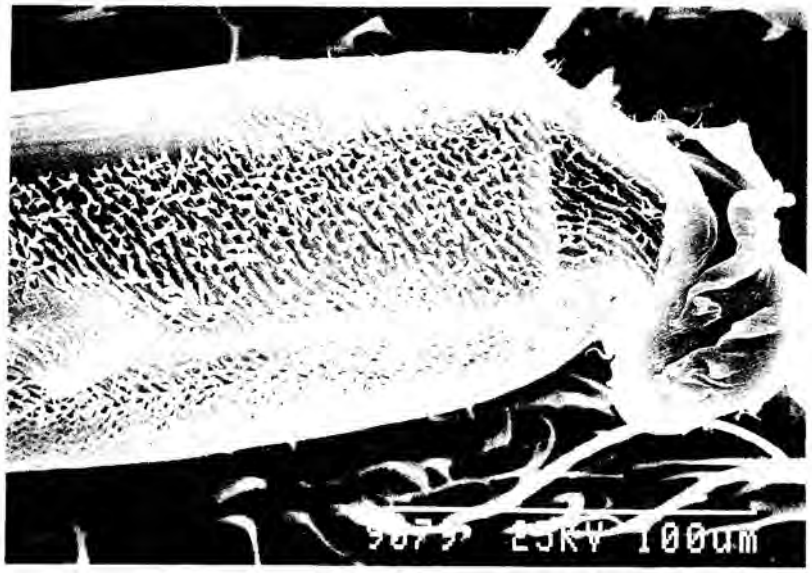

Figure 9: Birch with 0.1 g/sheet MA-PP, 0.3 MPa, 6 min., PP side of failure. Vessel casting. Note PP tendrils from pit field on the vessel casting (similar to figure 4).

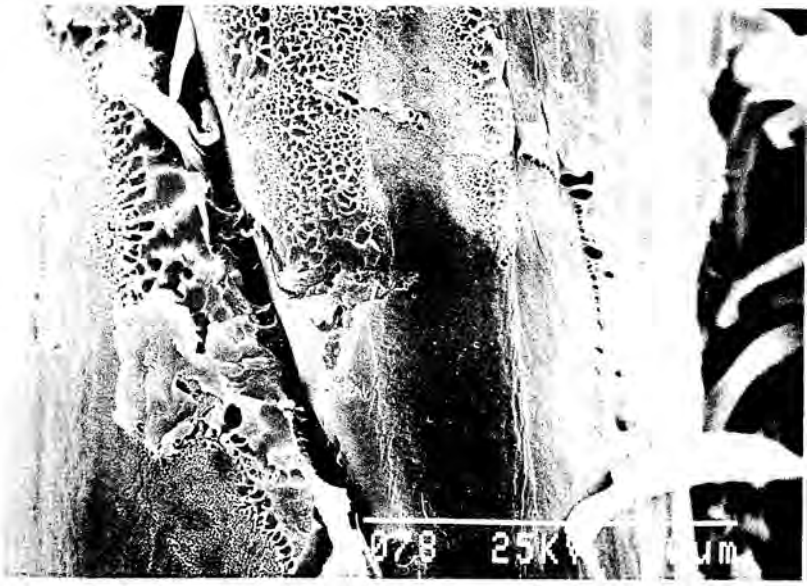

Figure 10: Birch with 0.1 g/sheet MA-PP, 0.3 MPa, 6 min., PP side of failure. Close-up of vessel casting. Note evidence of PP yielding indicating chemical adhesion to MA-PP.

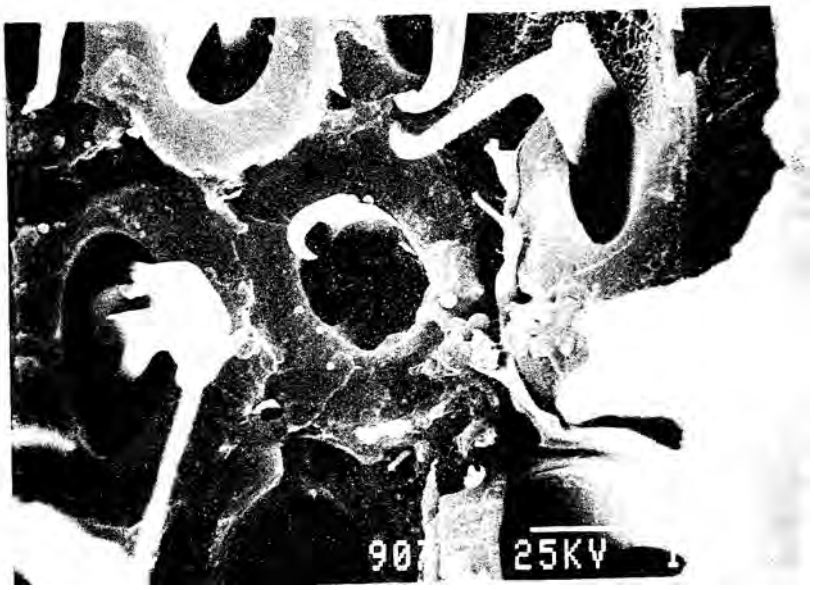

Figure 11: Birch with 0.1 g/sheet MA-PP, 0.3 MPa, 6 min., veneer side of failure. Ray cells. Note the coating on the ray cells, especially the center ray cell which is blocked.

Figure 12: Birch with 0.1 g/sheet MA-PP, 0.3 MPa, 6 min., PP side of failure. PP tendrils pulled from ray cells. Note similarity to figure 5.

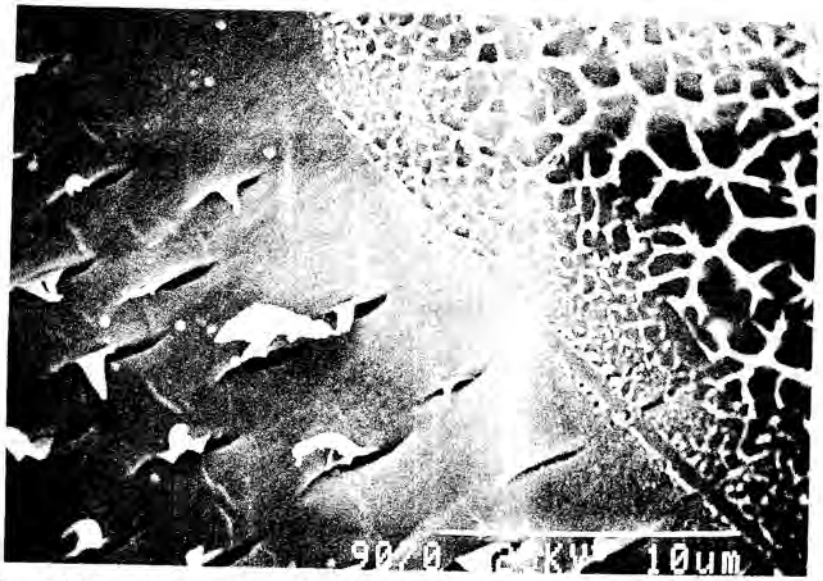

Figure 13: Birch with 0.1 g/sheet MA-PP, 0.3 MPa, 6 min., veneer side of failure. Coated pit field, region similar to figure 8. Note PP yielding indicating chemical adhesion to MA-PP (upper right corner).

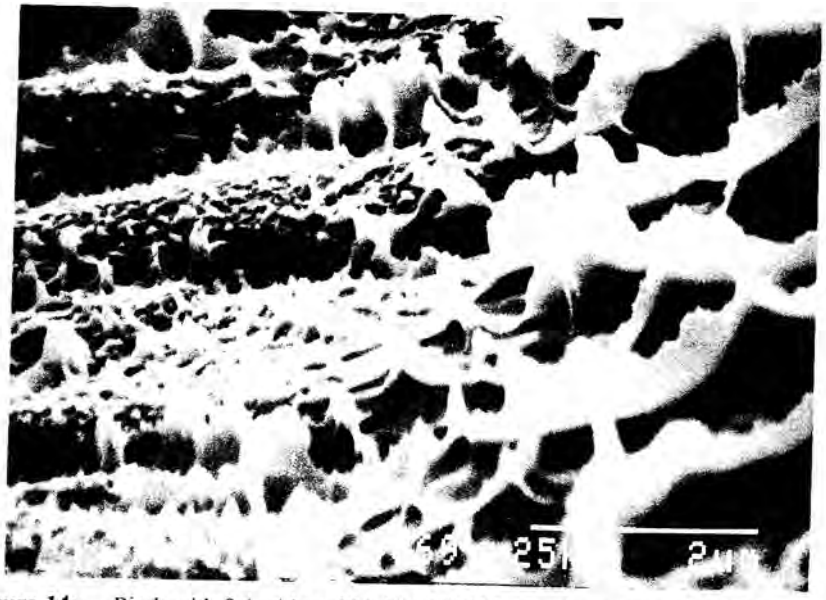

Figure 14: Birch with 0.1 g/sheet MA-PP, 0.3 MPa, 6 min., veneer side of failure. Close-up of PP yielding in region of chemical adhesion to MA-PP.

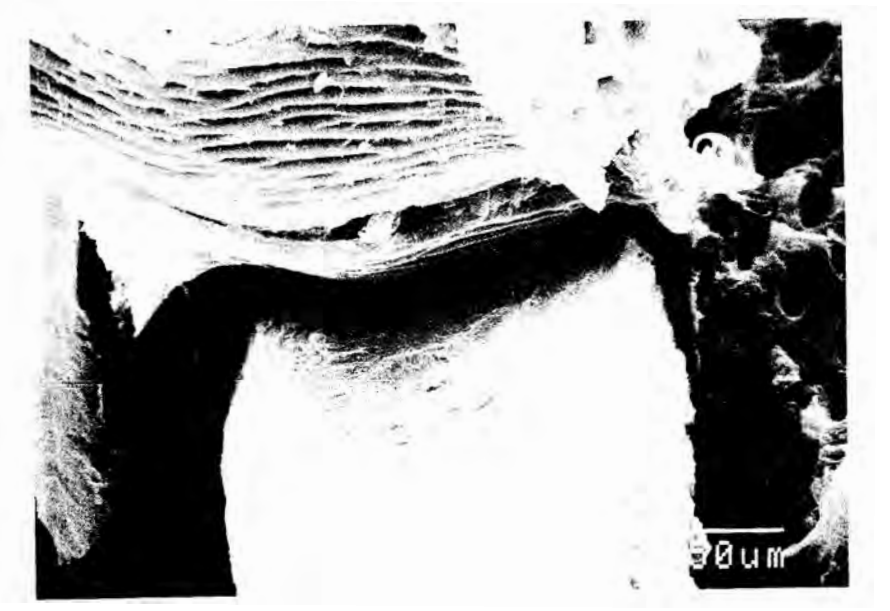

Figure 15: Birch with 1.5 g/sheet MA-PP, 0.3 MPa, 6 min., veneer side of failure. PP tendril extending from vessel opening. Note the absence of pit tendrils.

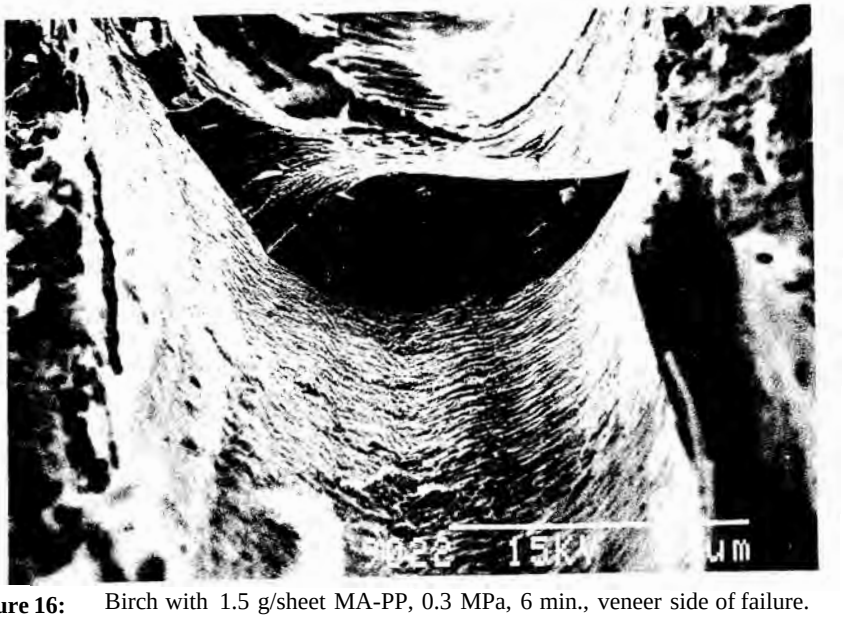

Figure 16: Birch with 1.5 g/sheet MA-PP, 0.3 MPa, 6 min., veneer side of failure. Low angle view of vessel. Note partial vessel blockage by MA-PP.

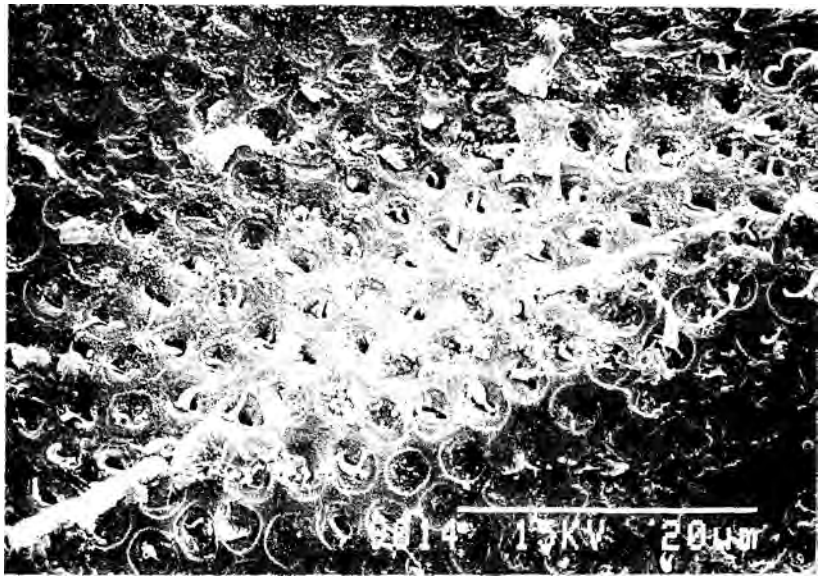

Figure 17: Birch with 1.5 g/sheet MA-PP. 0.3 MPa, 6 min., veneer side of failure. Coated pit field (outside of vessel) similar to figure 6. Note the nearly complete blockage of the pits by MA-PP.

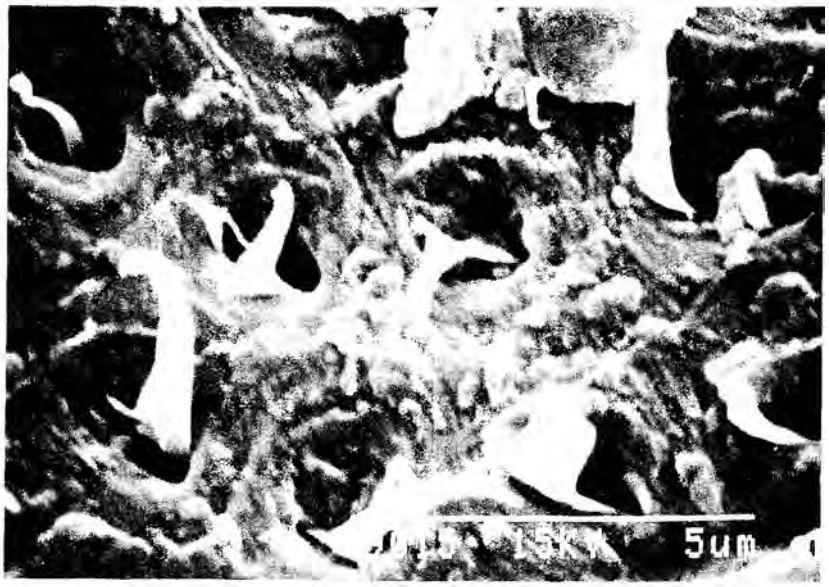

Figure 18: Birch with 1.5 g/sheet MA-PP, 0.3 MPa, 6 min., veneer side of failure. Close-up of figure 17. Note the MA-PP coating around the pits. Even the open pits are partially blocked.

Figure 19: Birch with 1.5 g/sheet MA-PP, 0.3 MPa, 3 min., PP side of failure. Vessel casting. Note complete absence of pit tendrils.

Figure 20: Birch with 1.5 g/sheet MA-PP, 0.3 MPa, 3 min., Veneer side of failure. Brittle failure plane in MA-PP layer.

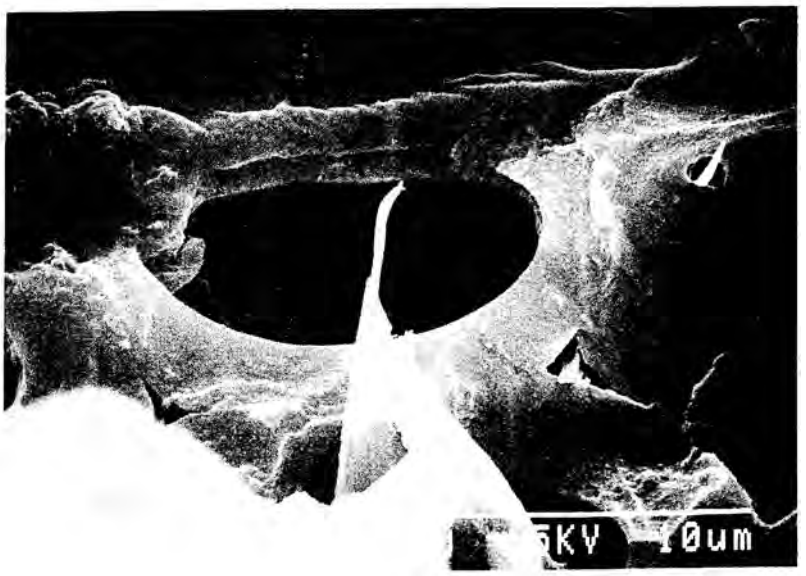

Figure 21: Birch with 1.5 g/sheet MA-PP, 0.3 MPa, 3 min., veneer side of failure. Coated ray cells. Note blockage inside ray cell.

Figure 22: Birch with 1.5 g/sheet MA-PP, 0.3 MPa, 3 min., PP side of failure. Ray cell casting by thick MA-PP layer. Note blunt nature of ray cell casting indicating brittle fracture and pull-out.

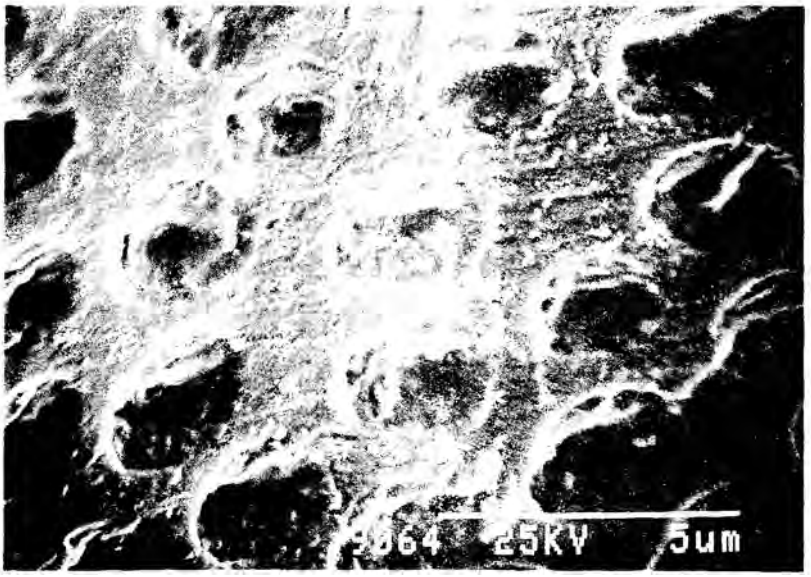

Figure 23: Birch with 1.5 g/sheet MA-FP, 0.3 MPa, 3 min., veneer side of failure. Coated pit field (outside vessel) similar to figure 6. Note complete blockage of pits by MA-PP.

Figure 24: Birch with 1.5 g/sheet MA-PP, 0.3 MPa, 3 min., veneer side of failure. Coated pit field (inside of vessel) similar to figure 8. Note partial blockage of vessel by MA-PP (right side of photo).

These observations indicate that MA-PP may interfere with mechanical adhesion between Birch and PP, while at the same time enhancing chemical adhesion. These two effects are greatly dependent on the MA-PP thickness. The importance of the thickness of the MA-PP layer is easily seen in the fracture surfaces. Very thick layers of MA-PP fail in the MA-PP layer. This failure is a weak, brittle failure. In the absence of MA-PP the PP failure is strong and ductile with evidence of significant yielding. The thickness of the MA-PP layer also controls the degree of blockage occurring in the various wood pores. The blockage of pores decreases the degree of mechanical adhesion of the PP to the wood. The decrease in mechanical adhesion also decreases the occurrence of yielding in the PP. Both of these effects can be offset by an increase in the chemical adhesion between MA-PP and wood and MA-PP and PP. This offsetting effect appears to be significant for the thinnest MA-PP layer investigated.

DSC RESULTS

Figure 25 shows evidence of PP crystal nucleation on untreated Birch surfaces, while the MA-PP treated surfaces exhibit crystallization similar to the pure PP. There is a slight shoulder on the treated Birch peak corresponding to the peak from the untreated sample. This shoulder can be attributed to the incomplete surface treatment of the Birch. This result suggests that the MA-PP coating on the wood surface inhibits nucleation of PP at the surface. The decrease in PP nucleation at the surface may decrease the mechanical adhesion.

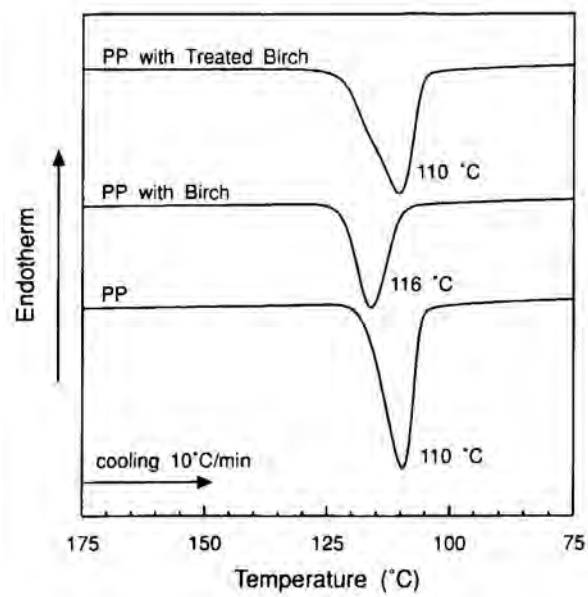

Figure 25 Differential Scanning Calorimetry Results. MA-PP treated Birch powder with polypropylene. PP crystallization peaks scanned from 200 °C to 50 °C at 10 °C/minute.

CONCLUSIONS

We propose an adhesive mechanism involving mechanical adhesion of PP to wood surfaces. In the absence of coupling agents or wood surface modification, the mechanical adhesion is the only contributor to the total adhesion. In the presence of MA-PP, both mechanical and chemical adhesion are present.

The mechanical adhesion appears to be decreased by the presence of MA-PP. This is mainly a result of preferential absorption of MA-PP, resulting in blockage of the pores available to the PP for mechanical interlocking. The effect of pore blockage should increase with increasing amounts of coupling agent. The MA-PP interference with PP nucleation may also play a role in decreasing mechanical adhesion.

The chemical adhesion appears to go through an effective maximum with increasing treatment level. This maximum is a result of the cohesive failure of the MA-PP layer as thickness increases.

The net result is the occurrence of an optimum MA-PP treatment level to increase the adhesion between PP and wood. This is illustrated schematically in figure 26. This maximum in adhesion should be a function of surface area and perhaps more importantly the pore size distribution of the wood species of interest.

This knowledge of the effects of MA-PP on adhesion suggest two avenues for improvement of the system, first, the use of MA-PP in quantities near the optimum treatment level and second, the use of maleated-polypropylenes of higher molecular weight. The latter would give an MA-PP layer with a higher toughness, thus reducing weak cohesive failure. Both of these suggestions should apply to wood flour- or wood fiber-filled systems as well as to the model laminate system studied here.

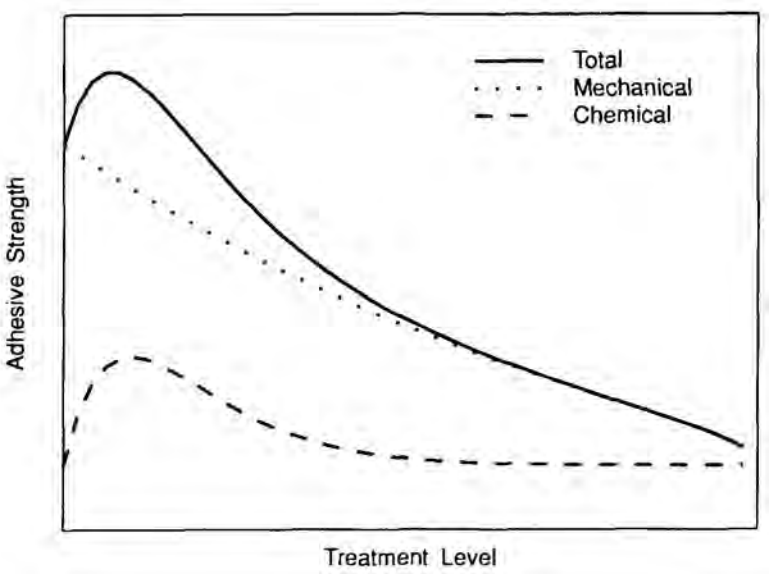

Figure 26 Theoretical contributions to total adhesion from mechanical and chemical adhesion.

1. G.-S. Han, S. Saka and N. Shiraishi, Mokuzai Gakkaishi 37, 241 (1991).
2. J.M. Felix and P. Gatenholm, J. of App. Pol. Sci. 42, 609 (1991).
3. A.M. Krzysik and J.A. Youngquist, Intern. J. of Adhesion and Adhesives. 11 (4), 235 (1991).
4. G.E. Myers, I.S. Chahyadi, C.A. Coberly and D.S. Ermer, Inter. J. of Pol. Mat. 15, 21 (1991).
5. D.J. Olsen in ANTEC '91 (Soc. of Plas. Eng., Inc., Tech. Papers 37, Montreal, ON, 1991) pp. 1886-1891.
6. P.C. Kolosick, C.T. Scott, J.A. Koutsky and G.E. Myers in Materials Interactions Relevant to the Pulp, Paper, and Wood Industries, edited by D.F. Caulfield, J.D. Passaretti and S.F. Sobczynski (Mater. Res. Soc. Proc. 197, San Francisco, CA 1990) pp. 119-124.

In: Rowell, Roger M.; Laufenberg, Theodore L.; Rowell, Judith K., eds. Materials interactions relevant to recycling of wood-based materials: Proceedings of Materials Research Society symposium; 1992 April 27–29; San Francico, CA. Pittsburg, PA: Materials Research Society; 1992: 137–154. Vol. 266.

Printed on Recycled Paper